Heliyon 10 (2024) e36231

Contents lists available at ScienceDirect

Heliyon

journal homepage: www.cell.com/heliyon

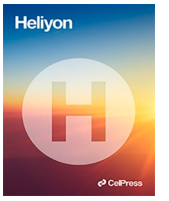

Research article

Insights into the molecular basis of gastric mucosa as a first step for using Raman microscopy in paediatrics

Jiří Bufka [a,b,1,*], Lenka Vaňková [c,1], Josef Sýkora [a], Magdaléna Daumová [d], Petr Bouř [b,**], Jan Schwarz [a]

[a] Department of Paediatrics, Faculty of Medicine in Pilsen, Faculty Hospital, Charles University in Prague, Pilsen, Czech Republic
[b] Institute of Organic Chemistry and Biochemistry, Czech Academy of Sciences Prague, Czech Republic
[c] Department of Histology and Embryology, Faculty of Medicine in Pilsen, Charles University, Czech Republic
[d] Sikl's Department of Pathology, Faculty of Medicine in Pilsen, Charles University, Czech Republic

ARTICLE INFO

Keywords:
Raman spectroscopy
Gaster
Mucosa
Measurement protocol
Diagnostic methods
Paediatrics

ABSTRACT

Recent advances in endoscopic technology have allowed detailed observation of the gastric mucosa, including Raman microscopy and spectroscopy. To explore the possibilities for future diagnostic use, we discuss the measurements and molecular markers found in this tissue. The Raman spectra of 16 samples of antral mucosa and 16 samples of corpus gastric mucosa obtained from healthy donors were analysed. A stable protocol for measuring reproducible spectra was established. These data suggest that many biomarkers can be used for the rapid analysis of metabolic states and future investigations into the pathogenesis of gastrointestinal diseases.

1. Introduction

Raman spectroscopy (RS) is a non-destructive analytical method based on the inelastic scattering of electromagnetic radiation by the molecules of a sample. Raman spectroscopy provides information on the geometry and vibrational states, and the Raman band frequencies and intensities reflect the molecular symmetry or chemical groups present [1,2]. In the past, multiple types of cellular metabolites have been characterised by this method, including amino acids, lipids, carbohydrates, nucleic acids, and carotenoids. In principle, each molecule has a unique spectral fingerprint [3,4]. Raman spectroscopy and microscopy have also been explored for many biomedical applications, including imaging the chemical composition of cells and tissues and analysing cellular metabolism [3–7]. RS appears to be a potentially useful diagnostic method and is also applicable to studies of molecular processes in the gastrointestinal system due to its non-invasiveness, adaptability, and speed of measurement.

The gastric mucosa, a layer of mucous membrane found in the stomach, performs multiple functions. Its epithelial cells secrete a thick and highly viscous mucus as a protective layer rich in bicarbonate ions [8]. Several cell types produce different metabolites. Thus, stomach malfunction is reflected in the different chemical compositions of the mucosa and mucus. This is normally evaluated using microscopic techniques. To the best of our knowledge, Raman spectroscopy has not yet been used for this purpose. First, we

* Corresponding author. Department of Paediatrics, Faculty of Medicine in Pilsen, Faculty Hospital, Charles University in Prague, Pilsen, Czech Republic, Alej Svobody 80, Pilsen, 323 00, Czech Republic.
** Corresponding author.
E-mail addresses: bufkaj@gmail.com (J. Bufka), bour@uochb.cas.cz (P. Bouř).
[1] These two authors contributed equally to this work.

https://doi.org/10.1016/j.heliyon.2024.e36231
Received 9 February 2024; Received in revised form 12 April 2024; Accepted 12 August 2024
Available online 14 August 2024

investigated the possibility of studying normal gastric cells using this technique. This is done under physiological conditions ("until the cell die"), which is another advantage compared to microscopy, where rather complex fixation and staining must be used. It should also be stressed that, in our case, Raman analysis did not imply an additional burden for the patients since the stomach tissue samples were already taken for other purposes. In contrast, in vivo measurements may completely replace biopsy in the future, significantly reducing the stress associated with the examination.

2. Material and methods

2.1. Sample collection

Stomach tissue samples were obtained from paediatric patients in the Division of Gastroenterology, Department of Paediatrics, University Hospital, Pilsen. Patients (aged 3–18) underwent upper gastrointestinal endoscopy (UGE) from 9/2023 to 1/2024 and were diagnosed with normal gastric mucosa. The samples were also investigated using classical histological techniques, and unhealthy antral and corpus gastric mucosae were excluded. Strict inclusion and exclusion criteria were applied. The indications for UGE were various gastrointestinal complaints suggestive of pathological conditions of the upper digestive tract, such as eosinophilic oesophagitis (EoE), celiac disease (CS), reflux oesophagitis, gastroesophageal reflux (GER), and inflammatory bowel disease (IBD), or percutaneous endoscopic gastrostomy (PEG). The exclusion criteria were as follows: (1) insufficient biopsy samples for pathological examinations; (2) antibiotics, anti-H_2, proton pump inhibitors (PPIs), or nonsteroidal anti-inflammatory drugs (NSAIDs) administered 4 weeks before UGE; and (3) previously treated *H. pylori* infection.

During UGE, mucosal biopsies were obtained from the gastric antrum (angular incisure, $n = 2$) and corpus (centre of the greater curvature, $n = 2$) using large cup forceps.

The biopsy forceps currently available on the market are equally efficient in providing a histological diagnosis regarding the depth of the acquired specimen (lamina propria, lamina muscularis mucosae, and tunica submucosa).

For comparison, samples were collected from approximately the same location in the stomach. One biopsy sample was used for immediate measurement on a Raman microscopy; the process is schematically visualised in Fig. 1. The other gastric samples were fixed in 10 % neutral formalin, embedded in paraffin, sectioned at 5 μm, and stained with haematoxylin and eosin (H&E) for conventional histopathological analysis, according to the modified Sydney classification [9]. Biopsy samples were evaluated by an experienced pathologist in a blinded manner (Figs. 2 and 3). The features of the gastric mucosa (amount and activity of inflammation, lymphocyte and neutrophil granulocyte infiltration, atrophy, metaplasia, hyperplasia, and presence of *Helicobacter pylori*) were analysed and

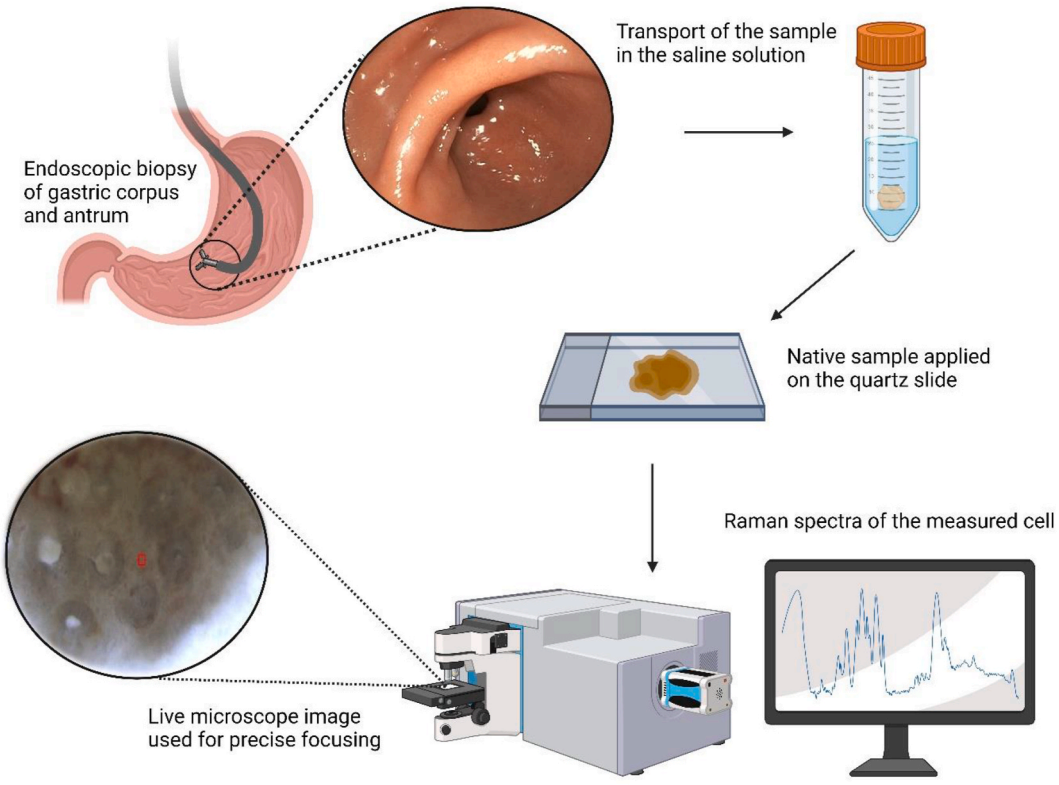

Fig. 1. Sample preparation and the measurement of Raman spectra.

graded using the visual analogue scale given in the modified Sydney classification, which is the most widely applied clinical protocol, as previously described [9].

All patients enrolled in this study received a summary score of 0, with a maximum score of 1, on the histopathological evaluation of the samples. Grade 1 was only acceptable in the first category, cellularity, exhibited by 6 out of 16 patients, and other scores (inflammatory activity, atrophy, intestinal metaplasia, and *Helicobacter pylori*) were 0 for all patients.

2.2. Spectra measurement

The biopsy material was placed in 0.90 % w/v NaCl, anonymised at the time of sampling, immediately transported to the microscopy laboratory, and transferred to a quartz glass slide. The transport time from biopsy to measurement was less than 15 min. If necessary, an additional saline solution was added to prevent the sample from drying. Raman spectra were recorded on a Raman microscope (Olympus, Japan) equipped with a Raman spectrometer (DXR1, Thermo Scientific, USA) using a 10 × objective (Olympus, Japan) and a diode laser beam (wavelength 532 nm, power 6.5–7 mW). The signal came from a spot of approximately 50 μm in diameter, comprising about one cell. Under the laser power used, no cellular damage was observed during measurements. In the microscope, the objective lens collects backscattered light from the sample, which is filtered using a holographic notch filter and directed to the spectrometer and charge-coupled device (CCD) detector. The measurements were completed within 35 min from the time of the biopsy. Thus, the current signal-to-noise ratio is a compromise between the spectral accumulation time and sample stability, neither of which can be significantly varied.

Cells were selected using the standard visual mode of the microscope, and at least five cells were measured for each sample. Raman spectra were processed using Olympus and our software; the fluorescence background was subtracted; and the positions of the strongest Raman peaks were determined using a polynomial fit at the local maxima. The peaks were assigned based on the literature data.

An example of baseline fitting and the spectra before and after subtraction are shown in Fig. 4. The background signal significantly distorts the measured spectra, and automatic baseline removal is a challenging problem in Raman spectroscopy [3]. In our case, the algorithm described in Fig. 4 worked reasonably well. However, the relative band intensities may contain an error of approximately 10 % owing to imperfect background removal.

2.3. Ethics statement

Informed consent for the use of the biological material for research purposes was obtained according to the protocol approved by the Ethics Committee of University Hospital Pilsen and Faculty of Medicine in Pilsen, Charles University, on 31 August 2023 with Reference Number 324/23. A biopsy of the gastric mucosa was performed endoscopically. Biopsies were performed by the Department of Paediatrics, University Hospital in Pilsen, according to the institutional guidelines.

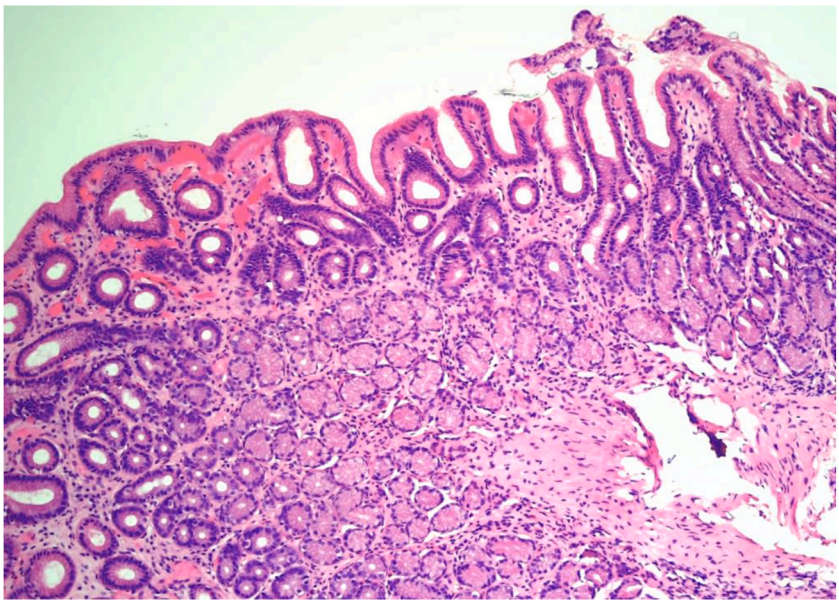

Fig. 2. Biopsy of antral mucosa containing surface epithelium, lamina propria and part of lamina muscularis mucosae (H&E, 100×).

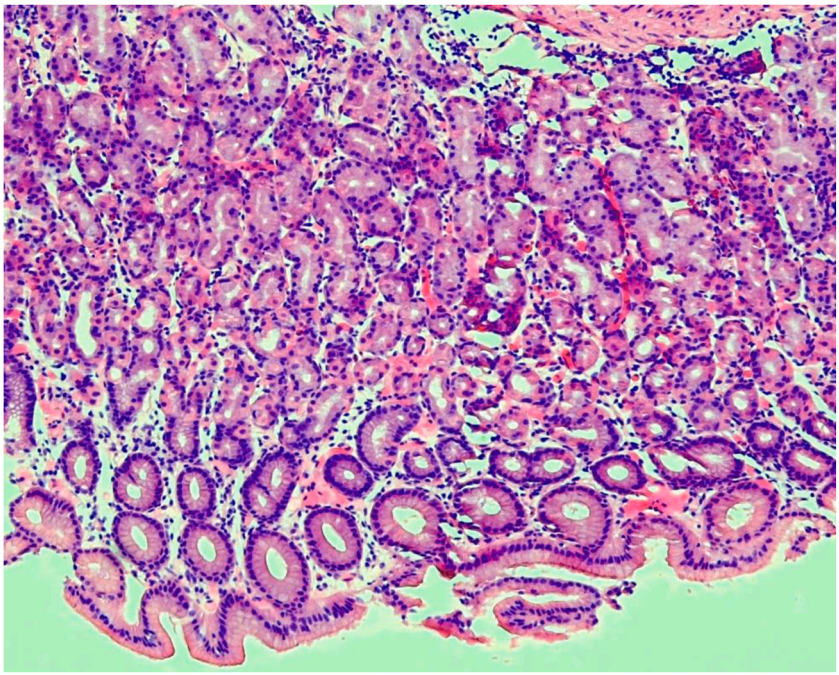

Fig. 3. Biopsy of corporal mucosa containing surface epithelium, lamina propria and part of lamina muscularis mucosae (H&E, 100×).

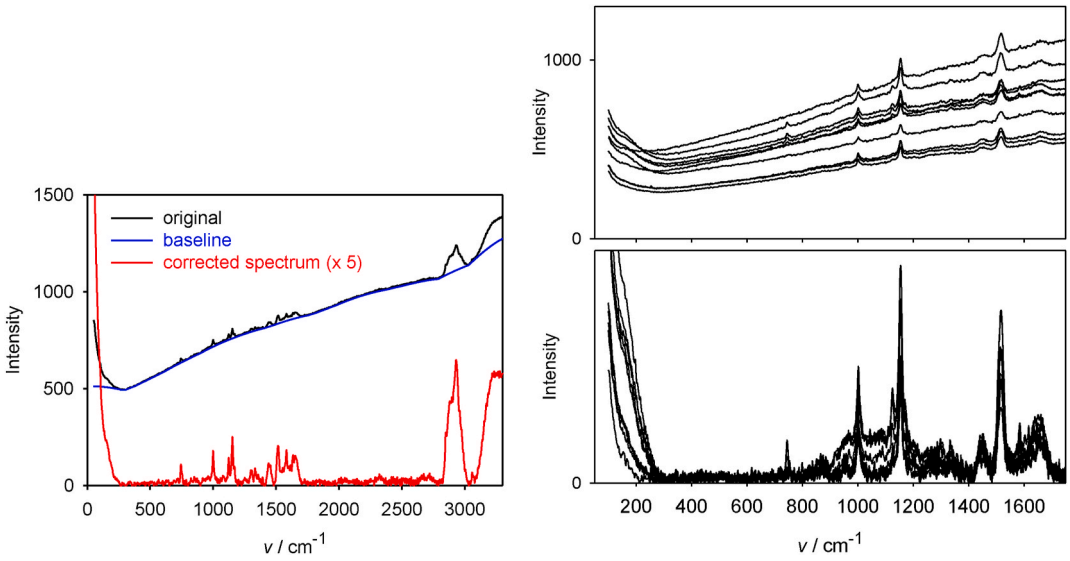

Fig. 4. Left: Example of a spectrum and an automatic baseline correction. The algorithm included three steps. 1) Load spectrum S; save in S_0. 2) Make new spectrum with points $S'_i = \min [(S_{i-1} + S_{i+1})/2 + a, S_{0i}]$. 3) go to 2) until convergence. The parameter a is chosen empirically. Right: Randomly chosen 10 Raman spectra of healthy antral gastric cells before and after baseline processing.

3. Results and discussion

We measured the spectra of the 16 healthy donors. As mentioned above, the spectra were accompanied by strong residual fluorescence, which was highly dependent on the actual sample. We also observed that damaged samples/unhealthy tissues produced a higher fluorescent background; however, this aspect is beyond the scope of the present study. Fortunately, for the investigated samples, most of the background fluorescent signals could be subtracted, and the resultant spectra varied significantly (Fig. 4). For the averaged spectra, the positions of the main peaks are shown in Fig. 5, and the assignments are listed in Table 1. The spectra were not normalised; the intensities were comparable because of averaging, and the same protocols were used for the samples from the two

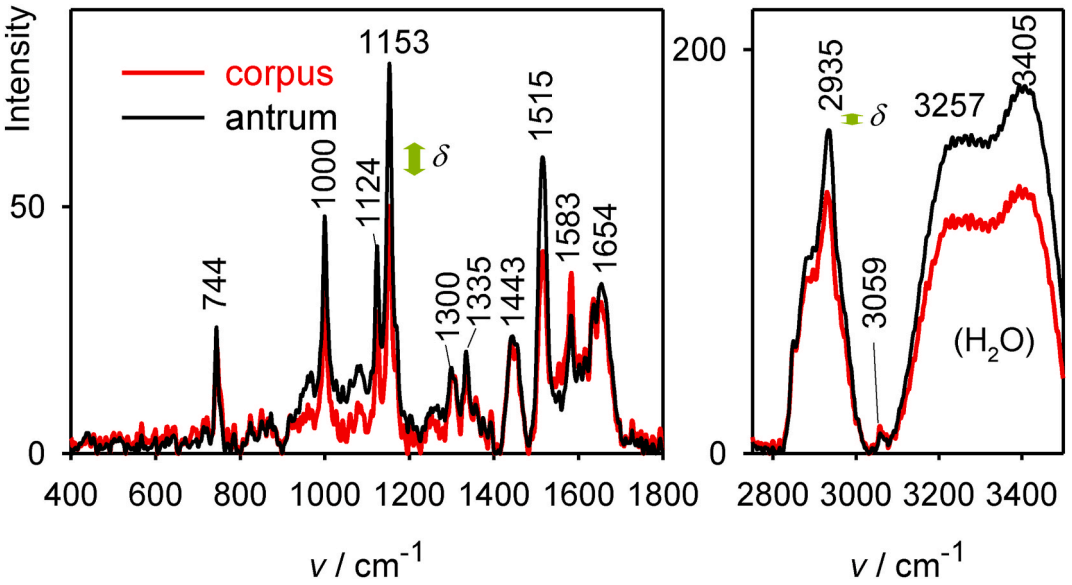

Fig. 5. Average Raman spectra of healthy gastric cells from the antral and corpus stomach parts, positions of the strongest bands, δ is the error of average intensity (approx. 7 in both spectral ranges for the biggest bands, corresponding to a root mean square error of ~33).

Table 1
Bands indicating the presence of some biomarkers.

	Carotenoids	Proteins	Lipids	Nucleic acids	Cytochrome C	Aromatic compounds
ν/cm^{-1}	1000, 1153, 1515	438, 1082, 1583, 1654	2935 (CH stretch)	744, 785, 1335, 1443	1124	3059

stomach parts. A formal error of the average intensity is indicated (~7 in all instrumental units displayed), which is relatively small; however, the actual uncertainty may be larger owing to baseline subtraction and other factors.

For compounds likely to be present in the tissues, bands of carotenoids (1000, 1153, and 1515 cm^{-1}), proteins (438, 1082, 1583, and 1654 cm^{-1}), lipids (2935 cm^{-1}), nucleic acids (744, 785, 1335, and 1443 cm^{-1}), cytochrome C (1124 cm^{-1}) and aromatic compounds (3059 cm^{-1}) are visible [4,10–15]. The spectra of the mucosa in the antrum and corpus (Fig. 4) were similar, although there were minor differences, such as in the intensity of the CH stretching signal (~2930 cm^{-1}). This indicates differences in lipid content and other cellular components between the two sample types. Factor analysis was performed on the spectral set; however, to date, statistical processing has not provided useful data because of the experimental noise, limited number of samples, and fluorescent background.

Nevertheless, the richness of the spectra indicates the potential of Raman spectroscopy to study biochemical processes in the normal gastric mucosa and its subcellular metabolomics. The spectra were dominated by the vibrations of carotenoids and other components, including proteins and lipids. Although carotenoids and cytochrome C may be present at lower concentrations than other components, the signal is enhanced owing to the pre-resonance conditions when the absorption bands of these dyes are close to the 532 nm laser excitation. Carotenoids, which are known for their antioxidant properties, structure, and concentration, vary significantly between healthy and damaged cells and thus probably have the greatest potential for diagnostic purposes [16–20].

Carotenoids, cytochrome C, and protein contents can also be regulated by intrinsic biosynthesis pathways for energy production and other metabolic processes in the mitochondria. Particularly, they participate in antioxidant events and induce intercellular communication via gap junctions [17–22].

Thus far, we have not attempted extensive mapping except to collect spectra from similar tissue regions. The lower magnification (10 × objective) and aperture cause a smaller spatial resolution but enable the integration of the signal from more materials, thus leading to better reproducibility of the spectra. Another limitation of our study is the small number of samples (~200 spectra, 16 donors) given, among other reasons, strict criteria for patient selection. The number of measurements from a single sample was relatively low because of the limited lifespan of the cells (<30 min). Even within this period, some variability in the spectra can be attributed to the state of the cells, from fully fresh to dying. Their discrimination in native samples using standard microscopy is difficult. Another limitation for future healthy/damaged cell studies could be the diversity of cells and their spectra in healthy gastric mucosa, obscuring the differences needed for diagnosis. Additionally, despite our efforts, we could not be sure whether we always measured the same type of cell. The amount and composition of the protective mucus present in the mucosa, although we tried to wash it, can also contribute to the spectral variability. However, objective Raman data may detect many changes, such as extragastric pathologies, that cannot be detected by histopathological evaluation.

4. Conclusion

We established a protocol for obtaining, processing, and measuring the tissue samples for Raman spectroscopy. Band assignment demonstrated the feasibility of utilising Raman microscopy to describe the molecular composition of the normal gastric mucosa and identify molecular fingerprints. The most prominent Raman bands in normal antral cells were at 744, 1000, 1124, 1152, 1515, 1654, and 2935 cm^{-1}, and those in normal corpus cells 744, 1000, 1124, 1153, 1583, 1654, and 2932 cm^{-1}. Carotenoids and cytochrome C likely supplied the strongest signals, followed by lipids and proteins. The results indicated good reproducibility and low inter-individual variability in the spectral parameters. Thus, Raman spectroscopy has the potential to classify normal gastric mucosa with high accuracy and is susceptible to future automation and extension to other parts of the gastrointestinal mucosa, particularly those with pathological states.

Ethics statement

The study was reviewed and approved by the Ethics Committee of the University Hospital Pilsen and Faculty of Medicine in Pilsen, Charles University, on August 31, 2023, with Reference Number 324/23. Informed consent was obtained for the use of the biological materials for research purposes.

Funding information

SVV Grant No. 260 651, Grant Agency of the Czech Republic (22-04669S) and the Cooperatio programmes supported this work.

Data availability statement

The datasets generated and analysed in the current study are available from the corresponding author upon request.

CRediT authorship contribution statement

Jiří Bufka: Writing – original draft, Visualization, Software, Methodology, Investigation, Data curation, Conceptualization. **Lenka Vaňková:** Writing – original draft, Visualization, Software, Investigation, Formal analysis, Conceptualization. **Josef Sýkora:** Writing – review & editing, Writing – original draft, Validation, Supervision. **Magdaléna Daumová:** Validation, Investigation. **Petr Bouř:** Writing – review & editing, Visualization, Validation, Supervision, Software, Formal analysis, Conceptualization. **Jan Schwarz:** Writing – review & editing, Validation, Investigation, Data curation.

Declaration of competing interest

The authors declare the following financial interests/personal relationships which may be considered as potential competing interests:Jiri Bufka reports article publishing charges was provided by Charles University Faculty of Medicine in Pilsen. If there are other authors, they declare that they have no known competing financial interests or personal relationships that could have appeared to influence the work reported in this paper.

Acknowledgements

We would like to thank prof. Jaroslav Hrabák from the Laboratory of Antibiotic Resistance and applications of Mass Spectrometry in Microbiology for permission to use the Raman spectrometer in his laboratory.

References

[1] L.D. Barron, Molecular Light Scattering and Optical Activity, second ed., Cambridge University Press, Cambridge, 2004.
[2] T. Wu, J. Kapitán, P. Bouř, Resolving resonant electronic states in chiral metal complexes by Raman optical activity spectroscopy, J. Phys. Chem. Lett. 13 (17) (2022) 3873–3877, https://doi.org/10.1021/acs.jpclett.2c00653.
[3] G. Schulze, A. Jirasek, M. Marcia, A. Lim, R.F. Turner, M.W. Blades, Investigation of selected baseline removal techniques as candidates for automated implementation, Appl. Spectrosc. 59 (5) (2005) 545–574, https://doi.org/10.1366/0003702053945985.
[4] Matanfack G. Azemtsop, J. Rüger, C. Stiebing, M. Schmitt, J. Popp, Imaging the invisible-Bioorthogonal Raman probes for imaging of cells and tissues, J. Biophot. 13 (9) (2020) e202000129, https://doi.org/10.1002/jbio.202000129.
[5] R.G. Parr, W. Yang, Density-functional Theory of Atoms and Molecules, first ed., Oxford University Press, Oxford, 1989.
[6] P. Bouř, J. Bufka, V. Křížková, et al., Raman spectroscopy, in: V. Křížková, P. Šigutová, M. Holubová, et al. (Eds.), Blood and Blood Components, Hematopoiesis, Selected Methods Used in Cytology, Histology and Hematology, Karolinum, Prague, 2021.
[7] G.W. Auner, S.K. Koya, C. Huang, B. Broadbent, M. Trexler, Z. Auner, et al., Applications of Raman spectroscopy in cancer diagnosis, Cancer Metastasis Rev. 37 (4) (2018) 691–717, https://doi.org/10.1007/s10555-018-9770-9.
[8] A.L. Mescher, Junqueira's Basic Histology Text & Atlas, sixteenth ed., McGraw Hill, 2021.
[9] M.F. Dixon, R.M. Genta, J.H. Yardley, P. Correa, Classification and grading of gastritis. The updated Sydney system. International workshop on the histopathology of gastritis, Houston 1994, Am. J. Surg. Pathol. 20 (10) (1996) 1161–1181, https://doi.org/10.1097/00000478-199610000-00001.
[10] W. Li, L. Wang, C. Luo, Z. Zhu, J. Ji, L. Pang, Q. Huang, Characteristic of five subpopulation leukocytes in single-cell levels based on partial principal component analysis coupled with Raman spectroscopy, Appl. Spectrosc. 74 (12) (2020) 1463–1472, https://doi.org/10.1177/0003702820938069.

[11] S. Managò, P. Mirabelli, M. Napolitano, G. Zito, A.C. De Luca, Raman detection and identification of normal and leukemic hematopoietic cells, J. Biophot. 11 (5) (2018) e201700265, https://doi.org/10.1002/jbio.201700265.
[12] M. Bahreini, A. Hosseinzadegan, A. Rashidi, S.R. Miri, H.R. Mirzaei, P. Hajian, A Raman-based serum constituents' analysis for gastric cancer diagnosis: in vitro study, Talanta 204 (2019) 826–832, https://doi.org/10.1016/j.talanta.2019.06.068.
[13] L. Shao, A. Zhang, Z. Rong, C. Wang, X. Jia, K. Zhang, R. Xiao, S. Wang, Fast and non-invasive serum detection technology based on surface-enhanced Raman spectroscopy and multivariate statistical analysis for liver disease, Nanomedicine 14 (2) (2018) 451–459, https://doi.org/10.1016/j.nano.2017.11.022.
[14] M. Hüttemann, P. Pecina, M. Rainbolt, T.H. Sanderson, V.E. Kagan, L. Samavati, et al., The multiple functions of cytochrome c and their regulation in life and death decisions of the mammalian cell: from respiration to apoptosis, Mitochondrion 11 (3) (2011) 369–381, https://doi.org/10.1016/j.mito.2011.01.010.
[15] W. Horn, H. Maier, A.J. Born, Reduction of cytochrome c by oral mucosa of patients with oropharyngeal cancer, Klin. Wochenschr. 66 (Suppl 11) (1988) 105–107.
[16] A. Milani, M. Basirnejad, S. Shahbazi, A. Bolhassani, Carotenoids: biochemistry, pharmacology and treatment, Br. J. Pharmacol. 174 (11) (2017) 1290–1324, https://doi.org/10.1111/bph.13625.
[17] J. Udensi, J. Loughman, E. Loskutova, H.J. Byrne, Raman spectroscopy of carotenoid compounds for clinical applications-A review, Molecules 27 (24) (2022) 9017, https://doi.org/10.3390/molecules27249017.
[18] D.R. Parachalil, J. McIntyre, H.J. Byrne, Potential of Raman spectroscopy for the analysis of plasma/serum in the liquid state: recent advances, Anal. Bioanal. Chem. 412 (9) (2020) 1993–2007, https://doi.org/10.1007/s00216-019-02349-1.
[19] Schut T.C. Bakker, G.J. Puppels, Y.M. Kraan, J. Greve, L.L. van der Maas, C.G. Figdor, Intracellular carotenoid levels measured by Raman microspectroscopy: comparison of lymphocytes from lung cancer patients and healthy individuals, Int. J. Cancer 74 (1) (1997) 20–25, https://doi.org/10.1002/(sici)1097-0215(19970220)74:1<20::aid-ijc4>3.0.co;2-2.
[20] S. McCutcheon, R.F. Stout Jr., D.C. Spray, The dynamic Nexus: gap junctions control protein localization and mobility in distinct and surprising ways, Sci. Rep. 10 (1) (2020) 17011, https://doi.org/10.1038/s41598-020-73892-6.
[21] M. Okada, N.I. Smith, A.F. Palonpon, H. Endo, S. Kawata, M. Sodeoka, K. Fujita, Label-free Raman observation of cytochrome c dynamics during apoptosis, Proc. Natl. Acad. Sci. U.S.A. 109 (1) (2012) 28–32, https://doi.org/10.1073/pnas.1107524108.
[22] L. Gao, H. Zhao, T. Li, P. Huo, D. Chen, B. Liu, Atomic force microscopy based tip-enhanced Raman spectroscopy in biology, Int. J. Mol. Sci. 19 (4) (2018) 1193, https://doi.org/10.3390/ijms19041193.